Author's Accepted Manuscript

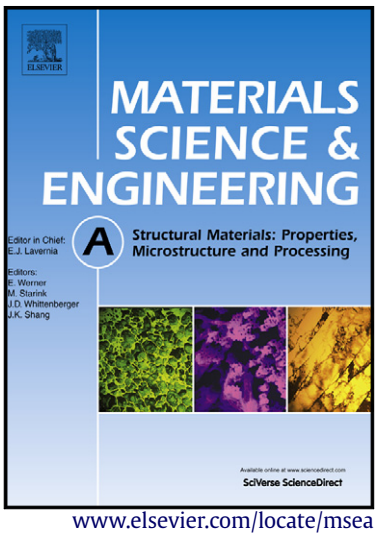

www.elsevier.com/locate/msea

Evolution of crystallite size, lattice parameter and internal strain in Al precipitates during high energy ball milling of partly amorphous $Al_{87}Ni_8La_5$ alloy

M. Dittrich, G. Schumacher

PII: S0921-5093(14)00263-9
DOI: http://dx.doi.org/10.1016/j.msea.2014.03.004
Reference: MSA30852

To appear in: *Materials Science & Engineering A*

Received date: 23 January 2014
Accepted date: 1 March 2014

Cite this article as: M. Dittrich, G. Schumacher, Evolution of crystallite size, lattice parameter and internal strain in Al precipitates during high energy ball milling of partly amorphous $Al_{87}Ni_8La_5$ alloy, *Materials Science & Engineering A,* http://dx.doi.org/10.1016/j.msea.2014.03.004

Evolution of crystallite size, lattice parameter and internal strain in Al precipitates during high energy ball milling of partly amorphous $Al_{87}Ni_8La_5$ alloy

M. Dittrich, G. Schumacher*

Helmholtz-Zentrum Berlin für Materialien und Energie GmbH, Hahn-Meitner-Platz 1, D–14109 Berlin, Germany

Abstract

The effects of plastic deformation by ball milling on the structure of a partly amorphous-$Al_{87}Ni_8La_5$alloy were investigated by X-ray diffractometry. Lattice parameter, crystallite size and lattice strain of the fcc-Al precipitates were determined by Rietveld refinement, double-Voigt approach and Williamson-Hall plots. The changes in lattice parameter of fcc-Al nano-precipitates during ball millingare ascribed tothe uptake of Ni. The crystallite size decreases as a function of the milling time from about 100 nm in the as-atomized state to about 14 nm after 1440 min of ball milling time. A modelbased on shear deformation of precipitates in the amorphous phase is used to describe quantitatively the decrease in crystallite size and change in lattice parameter.

Keywords:aluminum alloy, metallic glass, Al-TM-RE, plastic deformation, ball milling, shear deformation

*Corresponding author: Tel.: +49 30 8062 42400; fax: +49 30 8062 43059.

E-mail address: schumacher@helmholtz-berlin.de (G. Schumacher)

1 Introduction

Aluminum based metallic glasses (MG) exhibit good ductility combined with a higher strength compared to conventional aluminum based alloys [1]. At appropriate conditions, both thermal and mechanical treatment of Al based metallic glasses were shown to result in the formation of fcc-Al nanoprecipitates embedded in an Al-depleted amorphous matrix which results in improved mechanical properties compared to the single phase amorphous alloy prior to heat treatment[2]. Modifying the amount, size and morphology of the crystalline phase in the glass should, therefore, allow tailoring of the material properties of the alloy.

Structural analyses of Al-based MG after severe plastic deformation using different deformation techniques like cold rolling [3], high pressure torsion [4], equal channel angular pressing [5] and ball milling have been performed revealing the formation of fcc-Al nanoprecipitates in or close to shear bands. Only qualitative correlations between the degree of deformation and the structural changes were, however, found. For a better understanding of the deformation mechanisms in partly crystalline Al-based alloys a quantitative correlation between the degree of deformation and the changes in microstructure must be established. This work deals with severe plastic deformation of the partly amorphous $Al_{87}Ni_8La_5$ metallic glass which contains fcc-nanoprecipitates already in the as-atomized state. Plastic deformation is induced using a ball mill where the number of impacts between the balls in the mill and the powder particles can serve as a well-defined parameter for the deformation level. The changes in lattice parameter, internal strain and crystal size will be analyzed using X-ray diffractometry along with Rietveld refinement, William-Hall plots and a double Voigt approach. A qualitative model will be established to describe quantitatively the decrease in lattice parameter and crystal size as a function of the number of impacts between the balls in the mill and the powder particles.

2 Experimental

The alloywith nominal composition $Al_{87}Ni_8La_5$ (at.%) was synthesizedin an induction heat furnace under argon atmosphere using nearly pure elements Al (99.98 %), Ni (99.7 %) and La (99.7 %). The meltwasheated up to approximately 1200°Cand was subsequently atomized with helium gas using the Nanoval process [6].As reference material to the fcc-Al precipitates in the $Al_{87}Ni_8La_5$alloy, pure aluminum (99.97 wt%) annealed for 4h at 400°C was used for the XRD measurementin the unmilledstate and after 1440 min of ball milling time.

Ball milling was carried outwitha *Spex Mixer Mill 8000*. The powder container and two balls with 12.7 mm in diameter consist of zirconia. Milling was done under argon atmosphere for different milling times (60 min, 120 min, 240 min, 480 min, 960 min and1440 min).To avoid a temperature rise of the powder during milling, the mill was stopped for 45 min to cool downafter each 15 min of milling time.The differential scanning calorimetry (DSC) analysis has been done by means of a*Perkin-Elmer Pyris 1* calorimeter with a heating rate of 20 K/min and the transmission electron microscopy (TEM) by means of the*Philips CM30*.A TEM lamella was prepared by embedding the $Al_{87}Ni_8La_5$ powder in a special polymer.

Angle-dispersive XRD measurements on milled specimens were carried out by means of a *Bruker D8 Advance*diffractometer using Cu Kα radiation (wavelengthλ = 0.154 nm[7]). XRD patterns were analyzed in two ways.The first approach wasthe Rietveld refinement method implemented in *DIFFRACT^{plus}Topas 4.2*.The fundamental parameter analysis for the Rietveld refinement was done with the *NIST 660* XRD reference material. The background in the diffraction patternswasfitted withChebyshev polynomials and the broad halo from the amorphous phase was fitted with a “FP” type peak, which takes the diffractometerfundamental parameters and the amount of Lorentzian and Gaussian component of the peak shape into account. The identificationof aluminum Bragg peaks was done by determining the Bragg peak positions using the kinematic diffraction theory.For the determination of size and strain of the crystallitesthe double-Voigt approach[8]implemented in *DIFFRACT^{plus}Topas* 4.2 was used.The diffraction patterns from $Al_{87}Ni_8La_5$ revealed peaks with a minor Gaussian component.This amount could be reproduced by means of*OriginPro* with a Voigt fit resulting in full width at half maximum (FWHM) of$FWHM_{Gauss(111)} < 9{\cdot}E\text{-}5°$, and $FWHM_{Lorentz(111)} \approx 0.28°$ for the Gaussian and Lorentzian contributions, respectively. The step size of the XRD measurements was 2.77·E-2°.The Gaussian componentis practically not determinable.Therefore, it increased the standard deviation of the results (strain, crystallite size) drastically. It was necessary to deactivate the Gaussian component in the refinementto avoid meaningless parameters and error messages and this did notsignificantly affect the mean value significantly.

In the second approach, the crystallite size and lattice strain of the Al precipitates were determined by the Williamson-Hall plot[9]. TheWilliamson-Hall plotcombines the Scherrer equation (with a Scherrer constant of 0.9 according to Ref.[10]) and the lattice strain equation from Stokes & Wilson [11]. For this plot, the XRD pattern was Rachinger-($K\alpha_2$) and background-corrected.The Lorentz FWHM values were determined viapeak fitting by means of the analysis program *OriginPro*.The (400) reflections were not fitted because their intensity

was of the sameorder of magnitude as the background.The correction of the instrument broadening was done with the FWHM value of the Lorentz profile from the NIST 660 reference material. The crystallite size and strain were determined by the interception of the linear regression function with the vertical axis and the slope of a linear regression function which was calculated from the data in the Williamson-Hall Plot according to Ref.[9].

3 Results and discussion

In the as-atomized state,the $Al_{87}Ni_8La_5$ powder contains fcc-Al precipitates which are embedded in the Al depleted amorphous matrix, see Fig 1a. DSC measurements reveal an exothermic heat flow (≈ 0.05 W/g) at temperatures above 133 °C, see Fig 1b,whichis ascribed to structural relaxation within the amorphousphase. The first pronounced exothermic reaction was observed at the onset temperatureof 325 °C. This event was ascribed to the eutectic crystallization of Al_3Ni and $Al_{11}La_3$, as determined byXRD-analysis of a sample annealed at 355°C. In contrast to $Al_{85}Ni_{10}La_5$[12]where a pronounced exothermal reaction around 270°C has been observed and assigned to the formation of fcc Al crystals, such a pronounced exothermal heat flow could not be detected in the DSC diagram of $Al_{87}Ni_8La_5$. Furthermore, the XRD patterndid not reveal further crystallization of fcc-Al in$Al_{87}Ni_8La_5$ after annealing at 290°C. These results hint to a completely crystallized fcc-Al phase in the as-atomized state.

Plastic deformationof the $Al_{87}Ni_8La_5$powder by ball milling resulted in two characteristic changes in the XRD patternswhich are (i) a shift and (ii) broadening of all fcc-Al reflections, exemplarily shown for the (311) peak in Fig.2a. The peak shift is a result of changes in the average lattice parameter. It is generally caused by interstitials andoccupancy with impurity atoms, and can also depend on the crystallite size[13,14]. In the next section theshift and broadening of the fcc-Al reflections will be discussedin more detail.

3.1 Lattice parameter

The lattice parameter of the fcc-Al precipitates was determined by Rietveld analysis of the characteristic peak positionstaking into account the zero correction for the sample displacement, see Fig.2b. In the as-atomized state, the lattice parameter of the fcc-Al precipitates is identical to that of the aluminum reference material (a_{Al}= 4.050 Å). This suggeststhat in the as-atomized state the Ni and La concentrations in the fcc-Al precipitates are negligible.During ball milling the lattice parameter $a_{pr}$of the fcc-Al precipitates decreases from $a_{pr}(t = 0) = a_{Al}$= 4.050 Åto a_{pr}(t = 1440 min) =4.046 Å. This is in opposite direction to the change in the lattice parameter of the reference material which increases to $a_{Al}(t = 1440\ min)$= 4.052 Åafter

1440 min of ball milling time, see Fig. 2b.The different evolutionof the lattice parameter of the pure Al reference (+ 0.03 %) material and that of the precipitates (- 0.11 %) suggests that different mechanismsare responsible for the corresponding changes in lattice parameter during ball milling. While the change in the lattice parameter of pure aluminum is probably caused by self-interstitials and mechanically induced strains, the changes in the lattice parameter of the precipitates in $Al_{87}Ni_8La_5$are assigned to solid solution formation.The atomic radius of Ni (r_{Ni}=1.25 Å[15]is smaller compared to that of Al (r_{Al}= 1.43Å[15]) while the atomic radius of La (r_{La}= 1.88 Å[15]) is bigger. The decrease in the lattice parameter of the precipitates may,therefore,be ascribed to the preferred uptake of nickel in the crystal lattice of the fcc-Al precipitates during ball milling. Neglecting the possible uptake of La in the fcc lattice of the precipitates, the concentration of Ni in the fcc-Al phase $c_{(Ni)}$ can be estimated via Vegard'slaw[16]:

$$c_{Ni} = \frac{a_{Al} - a_{pr}}{a_{Al} - a_{Ni}} \quad (1)$$

where a_{Al}= 4.050Å [17]and a_{Ni}= 3.525 Å [18]denote the lattice parameters of pure Al and pure Ni, respectively.Based on the assumption that the lattice parameter is exclusively changed by the uptake of Ni,0.85% of Ni isdissolved in the fcc-Al precipitates after 1440 min of milling time. The uptake of La into the fcc-Al lattice would require a larger Ni concentration in the lattice to obtain the same change in the lattice parameter.According to Okamoto [19,20],both Ni and La arenotsoluble in fcc-Al.AlsoDan et al. [21]reported aminor solubility of 0.01% of Ni in Al at 640 °C in a binary Al-Ni phase system. This is not a contradiction to the present results because it is known that plastic deformation can dramatically enhance the solubility in binary systems (see, e.g., ref.[22]).Furthermore, the diffusion of alloying elements in metallic glasses is known to be sensitive to the relative size of the diffusing atoms and the host atoms [23]. Higher diffusivity of the smaller Ni compared to the larger La in the amorphous Al-based matrix supports the hypothesis of preferred uptake of Ni from the amorphous phase intothe Al crystallites during ball milling.

It has been reported that the lattice parameter increases or decreasesas a function of the crystallite size [14,24–27].There are several models which describe thecorrelationof the lattice parameter with the crystallite size based on (a) the surface energy [28–30], (b) the lack of the outermost bonding of the surface atoms [31],and (c) intra-crystalline pressure[32,33]. Accord-

ing to Qi et al. [14] the decrease in the lattice parameter ($\frac{a_{Al(t=0)} - a_{Al(t)}}{a_{Al(t=0)}} = \frac{\Delta a}{a_0}$)of aluminum-depends on the surface energy γ, thecrystallite shape α(α=1 for spherical shape), the shear modulus$G$and the crystallite size D.According to Qi et al. [14]the changes of the lattice parameter ($\frac{\Delta a}{a_0}$)of Al nanocrystals in ball milled $Al_{87}Ni_8La_5$can be described by

$$\frac{\Delta a}{a_0} = \frac{1}{1+\sqrt{\alpha}\cdot\frac{G}{\gamma}\cdot D} = \frac{1}{1+2.286E10\cdot D} \quad (2)$$

where the values of G and γ are taken from Ref.[14].The dashed line plotted in Fig. 3reveals the change of the lattice parameter ($\frac{\Delta a}{a_0}$) as a function of the crystallite sizecalculated with Eq. 2.

The measured lattice parameter of the precipitates (red dots inFig.3)neither follows the trend described by Eq. 2(dashed line in Fig.3) nor matches the results from Woltersdorf et al.[26] who found a strong increase in lattice parameter with decreasing particle size, see black square dots in Fig. 3. According to Fukuhara[31] the outermost bonds of the crystallite surface atoms are missing. Therefore, the missing-electrontobond-electron ratio increases if the crystallite size decreases,i.e., when the surface-to-volume ratio increases. In the $Al_{87}Ni_8La_5$ alloy fcc-Al crystallites are surrounded by an amorphous Albased matrix. Al atoms located at one side of the crystalline-amorphous interface will most probably be bonded to Al, Ni or La atoms at the other side of the interface. Interface effects between the crystallites and the amorphous matrix will, therefore, haveonly minor influence on the lattice parameter.

3.2 Lattice Strain and stress

Lattice strain and small crystallite sizes generally causepeak broadening in the diffraction pattern. Dislocations, incorporation ofimpurity atoms,antisite defects, micro- and macrostresses can contribute to the strain induced peak broadening[8,11,34]. The double-Voigt approach implementedin the Rietveld refinement(see Fig. 4a)and the Williamson-Hall plot(see Fig. 4b) are used todetermine the domain size and strain from the peak broadening. In the diffraction pattern (Fig. 4a) four peaks with high intensity and threepeaks with lower intensity are visible. An additionalWilliamson-Hall plot (WH4) was createdusing the high intensity peaks only. This procedure resulted in smallerdeviationsfromthe linear regression curve in

comparison with the Williamson-Hall plot created with seven peaks (WH7).As a result, the crystallite size and strain determined from the Williamson-Hall plots with four peaks (see Fig. 4c,d) is in better agreement withthe results from the double-Voigt approach thanthe William-son-Hall analysis with seven peaks.

The internal strain ε = 0.1 - 0.2 % in the precipitates in the as-atomized stateistwo orders of magnitude higher than the strainε= 0.002 % of the aluminum reference material. The strain analysis method is probably more sensitive to vacancies, impurities like Ar, and to solutes (Ni and La) in the fcc-Al lattice than the Rietveld analysis which revealed identical lattice parameter of the precipitates to that of the Al reference material in the initial state.That means the high strain in the fcc-Al precipitates in the as-atomized condition is presumably caused by defects like impurity atoms, self-interstitials or vacancies frozeninto the fcc-Al lattice during the gas atomization in contract to the (approximately) defect free annealed Al-reference material.As a result of plastic deformation, the strain in the precipitates strongly increases within the first 120 minutes of milling time toε = 0.3-0.4 %, depending on the type of analysis. WH4 and WH7 yield a decrease in strain in the fcc-Al precipitates upon further milling beyond t = 240 min while the double Voigt approach results in continuous increase in strain up to the maximum milling time, see Fig.4c. After 1440 min of ball milling time the strain ε = 0.045 %in the Al reference material is one order ofmagnitude lower than the strain ε = 0.30in the fcc-Al precipitates of $Al_{87}Ni_8La_5$. The internal stress σin the nanocrystalswas determined using the Young's Modulus (E = 72MPa[35]) of pure aluminumas an approximation of theYoung'smodulus of the fcc-Alprecipitates and using the experimentally determined values of the strain ε:

$$\sigma = \varepsilon \cdot E \qquad (3)$$

The maximum stress in the precipitates determined in this way is 226 MPa. This value is 3-6times larger than the tensile strength (40-80 MPa[35]) and larger by about a factor of 8-22compared tothe yield strength (10-30 MPa[35]) of pure aluminum. With Eq. 3 the internal stress of the reference material isdetermined to be 32 ± 6 MPa after 1440 min of milling time which is in agreementwith the values fromRef.[35].It is known from Ma et al. [36] that the Young's modulus in a metallic glass is similar to the Young's modulus of the crystalline phase of the main component of the metallic glass. The Young's modulus is generally not

very sensitive to small changes in the composition. It can, therefore, be assumed thatthe Young's moduli of the precipitates and of pure Al are about the same. This means that the Young's moduli of the fcc-Al precipitates and of the Al-based amorphous matrix in $Al_{87}Ni_8La_5$ alloy should be similar. Deformation induced stress in the amorphous phase of $Al_{87}Ni_8La_5$ alloy should, therefore, not lead to strain in the precipitates, which differsconsiderablyfrom the strainin the Al-reference material.It can, therefore,be concluded that thehigh strain-and stress values in the precipitates in the as-atomized state and after ball milling are mainly caused by impuritiesin the as-atomized state and by the uptake of Ni during ball milling, respectively.

3.3 Crystallite size

In the as-atomized state the crystallite size ***D*** determined by the double-Voigt and Williamson-Hall approach is in the range of 80 - 120 nm, see Fig. 4d. Within the first 480 minutes the crystallite size decreases strongly,then it tends to saturate. After 1440 min of milling time, the crystallite size decreased to $\boldsymbol{D} \approx 14$ nm. Hebert et al. [3]did not observe dislocations below the critical length scale of 11-18 nm of fcc-Al crystallites and deduced that dislocations are not stable below this critical crystallite scale.From this we conclude that dislocations do not contribute significantly to strain in the precipitatesafter 1440 minof milling time.Furthermore,according to Fig. 4c the strain stays nearly on the same level from 120 min to 1440 min of milling time, while the crystallite size decreases from around 100 nm to 14 nm. This leads to the conclusion that dislocation have no or only a minor influence on the average lattice strain during ball milling. It rather supportsthe assumption that the large internalstrain in the precipitates induced by ball milling is mainly chemically driven.

3.4 The model of fragmentation

Plastic deformation of metallic glasses proceeds via shear bands which are regarded as local areas of high strain in the amorphous matrix [37]. Ball milling induces shear bands in an amorphous powder particle at each impact. According to Liu [38] the orientation of the shear bands induced by ball milling is distributed randomly and the relative amount of shear band volume in a particle increases with increasing number of impacts, while the non-deformed volume content decreases. For crystalline materials, Maurice and Courtney [39] used the model of a particle with ductile binary layers (instead of crystallites) which wereplastically deformed by ball milling. In that model the thickness of the layers decreased exponentially as a function of the milling time (which is equivalent to the number of impacts). Based on dislocations in fcc-Al nanocrystals observed after cold-rolling, Hebert et al. [3] predicted a shear-induced fragmentation mechanism for precipitates ina partly amorphous Al-based metallic

glass. A study oflayered nanocomposites made out of crystalline Cu and amorphous Cu-Zr[40]reported the strain-induced formation of a homogeneous shear deformation zonethrough the layers. Shear band formation was also detected in the amorphous/nanocrystallinelayerof a Ti based composite material [41]. Based on these results it can beassumedthat ball milling deforms the $Al_{87}Ni_8La_5$powder particles via shear bands in the amorphous matrix. The shear bandstraversethe fcc-Al precipitates, leaving behind dislocations which cause fragmentation of the precipitatesand, therefore, crystallites of lower X-ray coherency length.A schematic depiction of the decrease in crystallite size during ball milling is shown in Fig. 5.

Similar to $Al_{85}Ni_{10}La_5$[38], the volume content of non-sheared material of the $Al_{87}Ni_8La_5$powder particle decreaseswith each impact. Starting with the initial crystallite size $\boldsymbol{D_0}$ in the as-atomized state, the amount of sheared crystallites increases and the average crystallite size $\boldsymbol{D}$ decreases exponentially as a function of the number of impacts $\boldsymbol{n}$ and approaches the saturation value $\boldsymbol{D_{sat}} = \boldsymbol{D(n = \infty)}$of the crystallite size. The decrease in crystallite size $\boldsymbol{D}$ as a function of $\boldsymbol{n}$ can be described by:

$$\boldsymbol{D(n) = \Delta D \cdot e^{\left(\frac{-n}{w}\right)} + D_{sat}} \quad \textbf{(4)}$$

where$\boldsymbol{\Delta D} = \boldsymbol{D_0} - \boldsymbol{D}_{\text{sat}}$ and $\boldsymbol{w}$ is the damping coefficient. The Spex Mixer Mill workswith a shaking frequency of $f = 17\ s^{-1}$, and the two balls (number of balls $\boldsymbol{n_B} = 2$) hit the powder twice a circle (once at the bottom and once at the top). Therefore, $\boldsymbol{n}$ can be calculated from the milling time $\boldsymbol{t}$bythe following equation:

$$\boldsymbol{n = 2 \cdot t \cdot n_B \cdot f} \quad \textbf{(5)}$$

The crystallite size $\boldsymbol{D}$as a function of $\boldsymbol{n}$along with a fit of equation (4) to the datais plotted in Fig. 6a. The value of the damping coefficient was determined to be$\boldsymbol{w} = (1.1 \pm 0.3) \cdot 10^6$ for the Williamson-Hall plotwith four peaks, $\boldsymbol{w} = (1.1 \pm 0.2) \cdot 10^6$for the Williamson-Hall plot with seven peaks, and $\boldsymbol{w} = (1.0 \pm 0.3) \cdot 10^6$ for the double-Voigt approach. Within the experimental uncertainty the values of $\boldsymbol{w}$arethe same for all three types of analyses. The satu-

ration value of the crystallite size is in the range of $\boldsymbol{D_{sat}}$= 13 - 15 nm for all three types of analysis.This saturation value is of the same order of magnitude as the shear band thickness (10 nm [42]) in Al-based glasses. In amorphous alloys crystallization occurs in or near the shear bands [42–45] caused by2 to 4 times higher diffusivity in the shear bands in comparison to the bulk material [46].Due to the high mobility of atoms in the shear bands,deformation induced formation of nanocrystals along with recrystallization of pre-existing precipitates is expected to occurin or near the shear bands.The saturation value of the crystallite size is, therefore, the result of at least two competing processes, fragmentation and crystallization of precipitates.Growth of pre-existing precipitates may also occur.The saturation value caused by fragmentation is determined by a critical crystallite size value below which dislocations are not stable. Further fragmentation during deformation is, therefore, no longer possible.The existence of even lower threshold values of crystallite sizes is known from plastic deformatio-nof pure crystalline metals [47]. Moreover,the saturation value of the crystallite size in $Al_{87}Ni_8La_5$is in agreement withHebert et al. [3] who could not observe dislocations below the critical length scale of 11-18 nmin fcc-Al crystallitesin cold-rolled $Al_{88}Y_7Fe_5$ metallic glass. At this length scale the crystallite size in $Al_{87}Ni_8La_5$will not be further reduced and will adopt its equilibrium size for infinitely large milling times.

Eq. (4) can be modified to describe the decrease in lattice parameter of the precipitates, $\boldsymbol{a_{pr}}$, by replacing the crystallite size with the lattice parameter:

$$\boldsymbol{a(n) = \Delta a_{pr} \cdot e^{\left(\frac{-n}{w}\right)} + a_{sat}} \qquad \textbf{(6)}$$

where$\boldsymbol{\Delta a_{pr}} = \boldsymbol{a_o} - \boldsymbol{a}_{sat,}\boldsymbol{a_o}$ and $\boldsymbol{a}_{sat}$ are the values of the lattice parameter of the precipitates at t = 0 and at t = ∞, respectively. Fitting Eq. 6 to the experimentally determined values of the lattice parameter,see Fig. 6b, results in$\boldsymbol{w}$ = (1.0 ± 0.1)·10^6 for the damping coefficient.The similarity of the values deduced from changes in crystallite size and from decrease in lattice parameter suggests that the same processes are responsible for the changes of these parame-ters.The exponential decay of the lattice parameter suggests a process in which certain volume fractions of the precipitates are completely saturated with Ni. When a particle is sheared due to an impact from a ball in the mill, the amorphous phase in the particle will be deformed by a shear band. For the sake of simplicity, it will be assumed that the deformation of the particle proceeds in a straight direction, i.e., the shear deformation penetrates the crystallite as shown in Ref.[40]. Similar to the glassy matrix, the deformation will cause a local increase in tem-perature in the Al precipitates near the shear deformation zone which allows the Ni atoms to

diffuse from the amorphous matrix into the shear deformed zone of the precipitate leading to local saturation of the Al-lattice in Ni within the precipitate.With increasing ball milling time the crystallite size decreases due to the increasing number of particle shear processes. Therefore, the amount of newly formed precipitate surface induced per impact decreases with increasing ball milling time. At large ball milling times, when the crystallite size remains constant,the deformation zones do not pass the precipitates and do not create newprecipitate surfaces. Hence, further uptake of Ni at shear surfaces of the precipitates does not occur any longerand the lattice parameter remains constant. This mechanism is still speculative and further research has to be done to clarify this point.

Liu [38] measured the decrease in the number of Al nearest neighbors around Ni and La atoms during plastic deformation of bulk amorphous $Al_{85}Ni_{10}La_5$ alloy with the same mill. He used a similar exponential lag function to describe the decrease of non-sheared volume inan amorphous powder particle during ball milling and found values of w which agree with the present values of w withina factor of less than 2. This supports the assumption that fccnanocrystals are sheared when shear bands traverse the powder particles. The comparison of our results with those of Liu [37] suggests that the present model is an extensionof Liu´smodel of increasing shear band volume in $Al_{85}Ni_{10}La_5$metallic glass to partly amorphous metallic glasses.

4 Summary and conclusions

Changes in lattice parameter, crystallite size and lattice strain of fcc-Al precipitates in partly amorphous $Al_{87}Ni_8La_5$ alloy during severeplastic deformation by ball milling were investigated by X-ray diffractometry. The data were analyzed by Rietveld refinement, double-Voigt approach and Williamson-Hall plot. It was observed that severe plastic deformation of partial amorphous $Al_{87}Ni_8La_5$ decreased the lattice parameter of the fcc-Al precipitates from 4.050 to 4.046 Å, that it decreased the crystallite size from 80 - 120 nm to ≈ 14 nm and increased the internal strain from $\varepsilon \approx 0.1$ % to $\varepsilon \approx 0.4$ % at large ball milling times of t = 1440 min. The analysis of the fcc-Al precipitates in the as-atomized state revealed a strain of $\varepsilon = 0.11\text{-}0.15\%$ which is two orders of magnitude larger than the strain in the pure Al reference material. Ball milling leads to a drastic increase in strain up to $\varepsilon = 0.28\text{-}0.43\%$ within the first 120 min of milling time. After 1440 min of ball milling time the strain is still one order of magnitude higher than the strain in the pure Al reference material. The result from the

strain and lattice parameter analysis implies that ball milling leads to the formation of an Al-Ni solid solution due to the uptake of Ni in the fcc-Al lattice.

A quantitative model was developed which describes the decrease in the crystallite size and change in lattice parameter during ball milling. The changes in crystallite size and change in lattice parameterwere described by the same model and resulted in damping coefficientsof similar size. This suggests that the uptake of Ni in the fcc-Al precipitates correlates with the fragmentation process.

Acknowledgements

The authors would like to thank N. Wanderka for help with the transmission electron microscopy, C. Förster for the specimen preparation and C. Leistner for help with differential scanning calorimetry experiments.

References

[1] A. Inoue, K. Ohtera, A.-P. Tsai, T. Masumoto, Jpn. J. Appl. Phys. 27 (1988) L479–L482.

[2] R.J. Hebert, Nanocrystals in Metallic Glasses, Nanocrystal, InTech 2011.

[3] R.J. Hebert, J.H. Perepezko, H. Rösner, G. Wilde, Scr. Mater. 54 (2006) 25–29.

[4] N. Boucharat, R.J. Hebert, H. Rösner, G. Wilde, Solid State Phenom. 114 (2006) 123–132.

[5] J. Vierke, G. Schumacher, M. Balog, J. Nagy, F. Simancik, M. Wollgarten, J. Banhart, Mater. Sci. Eng. A, 558 (2012) 64–69.

[6] L. Gerking, Powder Metall., 25 (1993) 59–65.

[7] B.B. He, Two-Dimensional x-Ray Diffraction, Wiley Hoboken, New Jersey, 2009.

[8] D. Balzar, in: R. Snyder, J. Fiala, and H. Bunge (Eds), Microstructure Analysis from Diffraction, Oxford University Press, New York, 1999, pp. 94–126.

[9] G.K. Williamson, W.H. Hall, Acta Metall. 1 (1953) 22–31.

[10] R. Allmann, Röntgen-Pulverdiffraktometrie, 2nd ed., Springer Berlin Heidelberg, 2003.

[11] A.R. Stokes, A.J.C. Wilson, Proc. Phys. Soc. 56 (1944) 174–181.

[12] Y. Liu, G. Schumacher, S. Zimmermann, J. Banhart, J. Alloys Compd.509 (2011) 78–81.

[13] C. Suryanarayana, Prog. Mater. Sci. 46 (2001) 1–184.

[14] W.H. Qi, M.P. Wang, J. Nanopart. Res. 7 (2005) 51–57.

[15] K. Lonsdale, International Tables for X-Ray Crystallography, Birmingham, England:, 1968.

[16] L. Spieß, G. Teichert, R. Schwarzer, H. Behnken, C. Genzel, Moderne Röntgenbeugung, Vieweg+Teubner, Wiesbaden, 2009.

[17] L. Kokot, R. Horyn, N. Iliew, J. Less Common Met. 44 (1976) 215–219.

[18] F. Wever, Z. Für Phys. 28 (1924) 69–90.

[19] H. Okamoto, J. Phase Equilib. 28 (2007) 581.

[20] H. Okamoto, J. Phase Equilib.14 (1993), pp. 257–259.

[21] B. Dan, C. Georgeta, A. Angel, Metal. Int. 11 (2006) 36–45.

[22] J.Z. Jiang, C. Gente, R. Bormann, Mater. Sci. Eng. 242 (1998) 268–277.

[23] F. Faupel, W. Frank, M.-P. Macht, H. Mehrer, V. Naundorf, K. Rätzke, H. Schober, S. Sharma, H. Teichler, Rev. Mod. Phys. 75 (2003) 237–280.

[24] M. Mhadhbi, M. Khitouni, L. Escoda, J.J. Suñol, M. Dammak, J. Nanomater. 2010 (2010) 1–8.

[25] S.A. Nepijko, E. Pippel, J. Woltersdorf, Phys. Stat. Sol. (a) 61 (1980) 469–475.

[26] J. Woltersdorf, A. Nepijko, E. Pippel, Surf. Sci. 106 (1981) 64–69.

[27] J. Sheng, U. Welzel, E.J. Mittemeijer, Appl. Phys. Lett. 97 (2010) 153109.

[28] C.W. Mays, J.S. Vermaak, D. Kuhlmann-Wilsdorf, Surf. Sci. 12 (1968), 134–140.

[29] C. Solliard, M. Flueli, Surf. Sci. 156 (1985) 487–494.

[30] R.C. Tolman, J. Chem. Phys. 16 (1948) 758–774.

[31] M. Fukuhara, Phys. Lett. A 313 (2003) 427–430.

[32] M.Y. Gamarnik, Phys. Stat. Sol. (b) 178 (1993) 59–69.

[33] M.Y. Gamarnik, Phys. Stat. Sol. (b) 164 (1991) 107–119.

[34] M. Herrmann, U. Förter-Barth, P.B. Kempa, Cent. Eur. J. Energ. Mater. 6 (2009) 183–193.

[35] W.W. Seidel, F. Hahn, Werkstofftechnik, 9th ed., Carl Hanser Verlag GmbH & Co. KG München, 2012.

[36] D. Ma, A.D. Stoica, X.-L. Wang, Z.P. Lu, B. Clausen, D.W. Brown, Phys. Rev. Lett. 108 (2012) 085501.

[37] A.L. Greer, Y.Q. Cheng, E. Ma, Mater. Sci. Eng. R 74 (2013) 71–132.

[38] Y. Liu, Local Structure of Al-Based Amorphous Alloys after Microalloying by Element Substitution and after Ball Milling, Technische Universität Berlin, PhD Thesis, 2011.

[39] D.R. Maurice, T.H. Courtney, Metall. Trans. A 21 (1990) 289–303.

[40] J.Y. Zhang, G. Liu, S.Y. Lei, J.J. Niu, J. Sun, Acta Mater. 60 (2012) 7183–7196.

[41] D.K. Yang, P. Cizek, D. Fabijanic, P.D. Hodgson, Mater. Sci. Eng. A 582 (2013) 162–169.

[42] A.A. Csontos, G.J. Shiflet, Nanostruct. Mater. 9 (1997) 281–289.

[43] W.H. Jiang, M. Atzmon, Acta Mater. 51 (2003) 4095–4105.

[44] W.H. Jiang, F.E. Pinkerton, M. Atzmon, Scr. Mater. 48 (2003) 1195–1200.

[45] N. Boucharat, R. Hebert, H. Rösner, R. Valiev, G. Wilde, Scr. Mater. 53 (2005) 823–828.

[46] J. Bokeloh, S. V. Divinski, G. Reglitz, G. Wilde, Phys. Rev. Lett. 107 (2011) 235503.

[47] H. Gleiter, Prog. Mater. Sci. 33 (1989) 223–315.

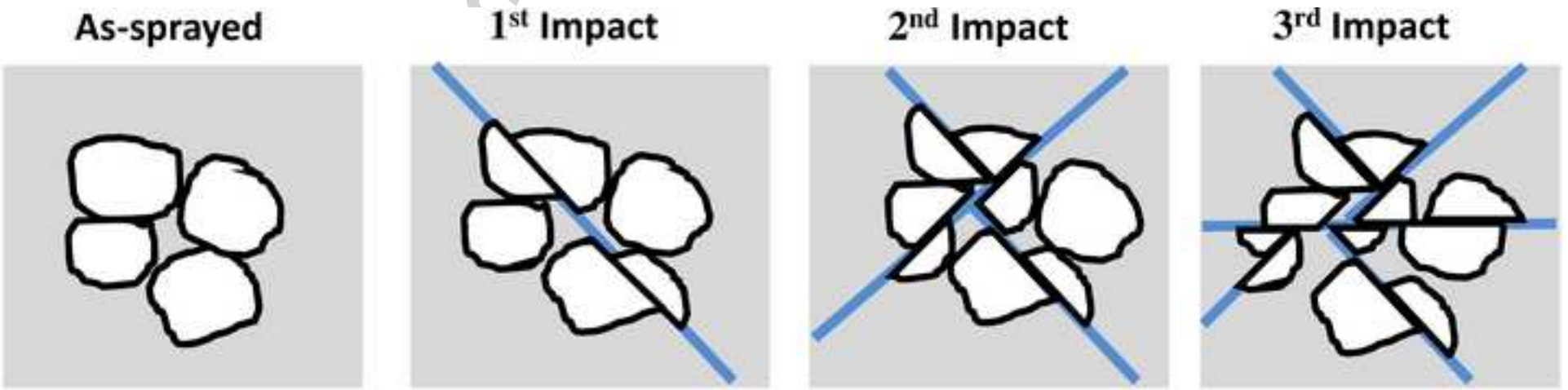

Figure 5: Schematic depiction of the crystallite size decrease. Precipitates (white) in the amorphous matrix (grey) are sheared by shear deformation zones (blue) during ball milling. The random orientation of the particle leads to shear deformation in random directions.

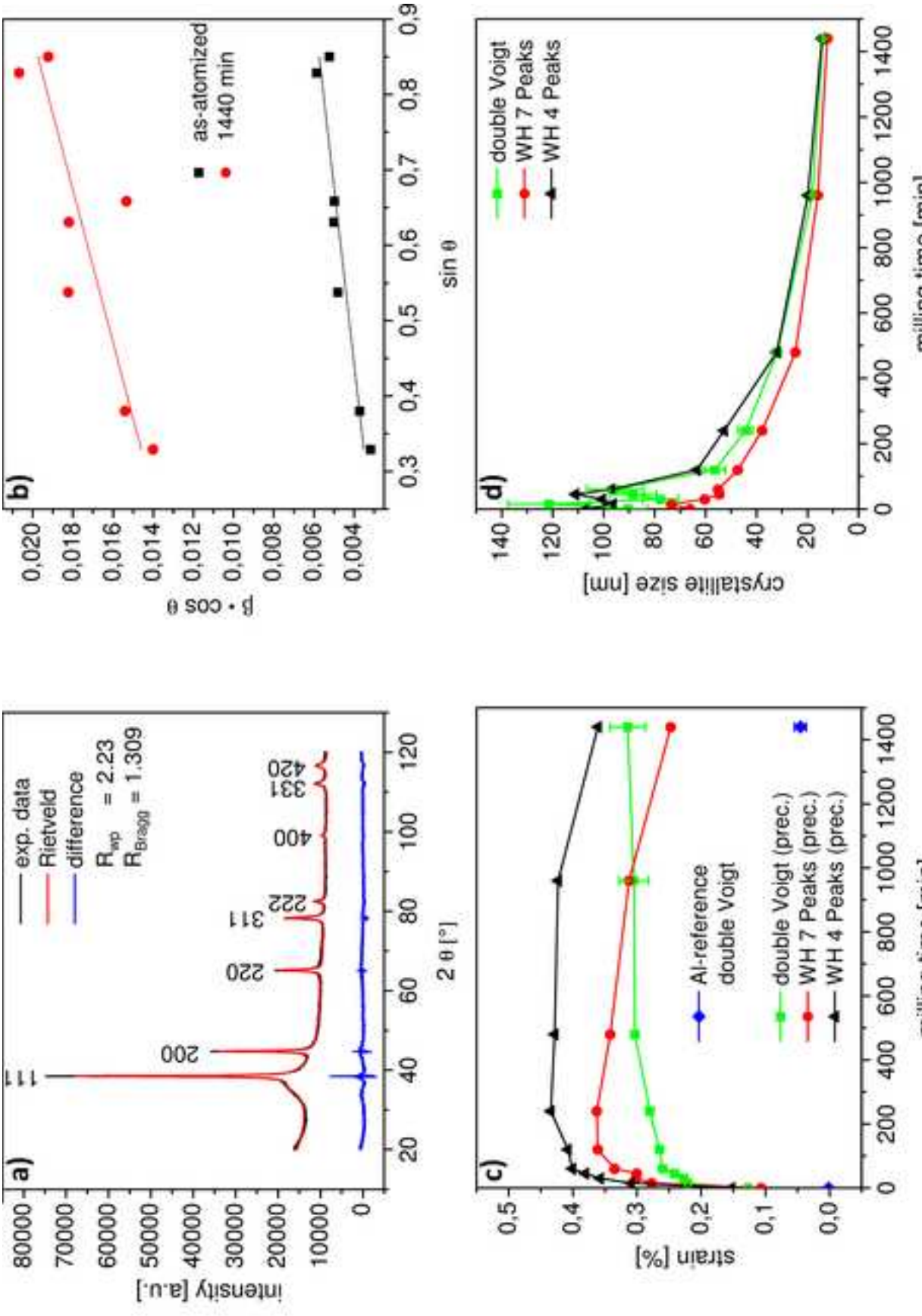

Figure 4: (a) XRD diffraction pattern of as-atomized $Al_{87}Ni_8La_5$ with the fitted refinement function and the corresponding fit quality R_{wp} and R_{Bragg}, (b) Williamson-Hall (WH) plot of as-atomized $Al_{87}Ni_8La_5$, (c) evolution of strain and (d) decrease of crystallite size determined by use of the double-Voigt and Williamson-Hall approaches as a function of ball milling time.

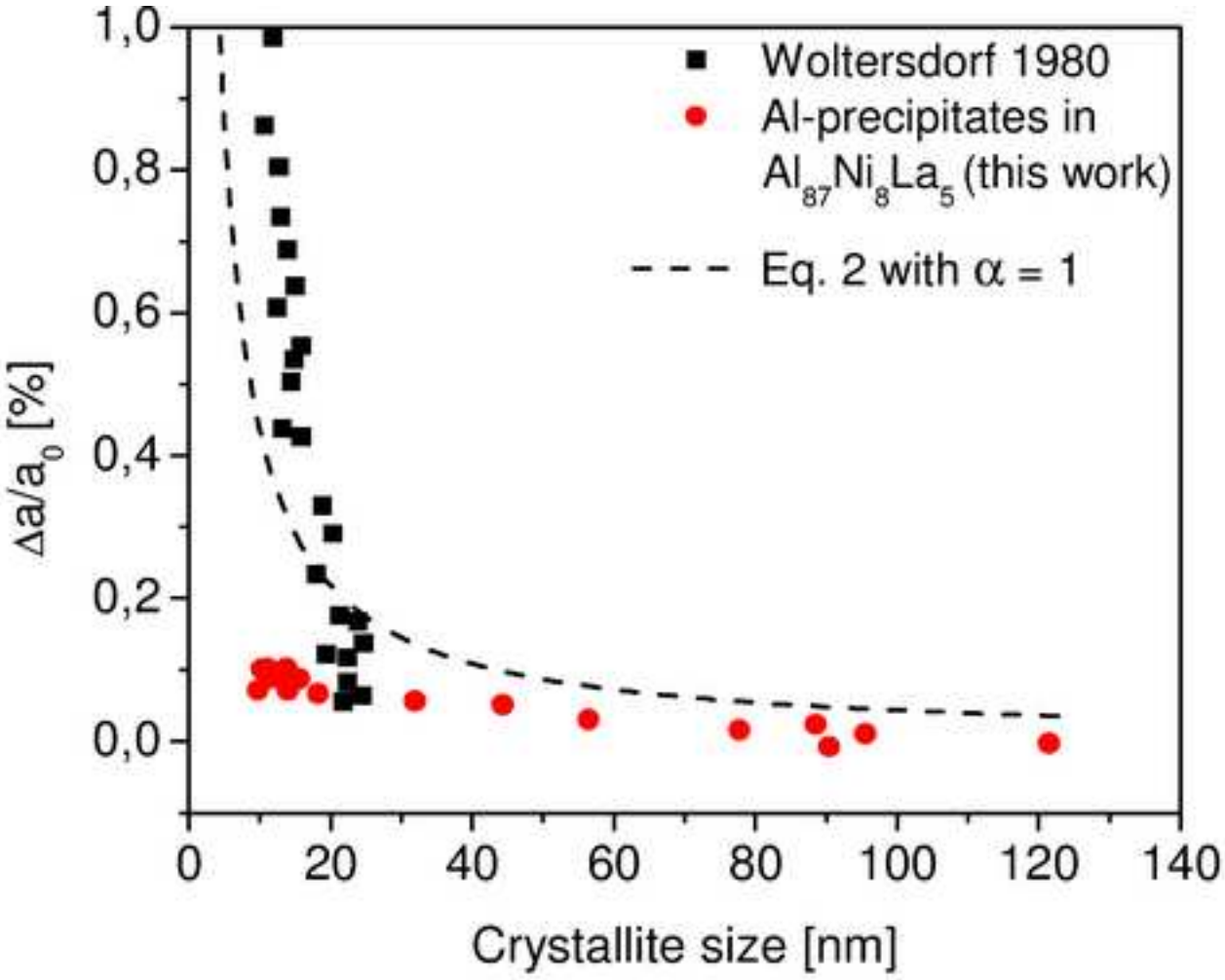

Figure 3: Change in the lattice parameter $(\frac{\Delta a}{a_0})$ as a function of the crystallite size. The dashed line is calculated from Eq. 2 with $\alpha = 1$, red dots belong to the fcc-Al precipitates in $Al_{87}Ni_8La_5$ (double-Voigt, Rietveld method), and black squares are values for Al crystallites reported in [50,51].

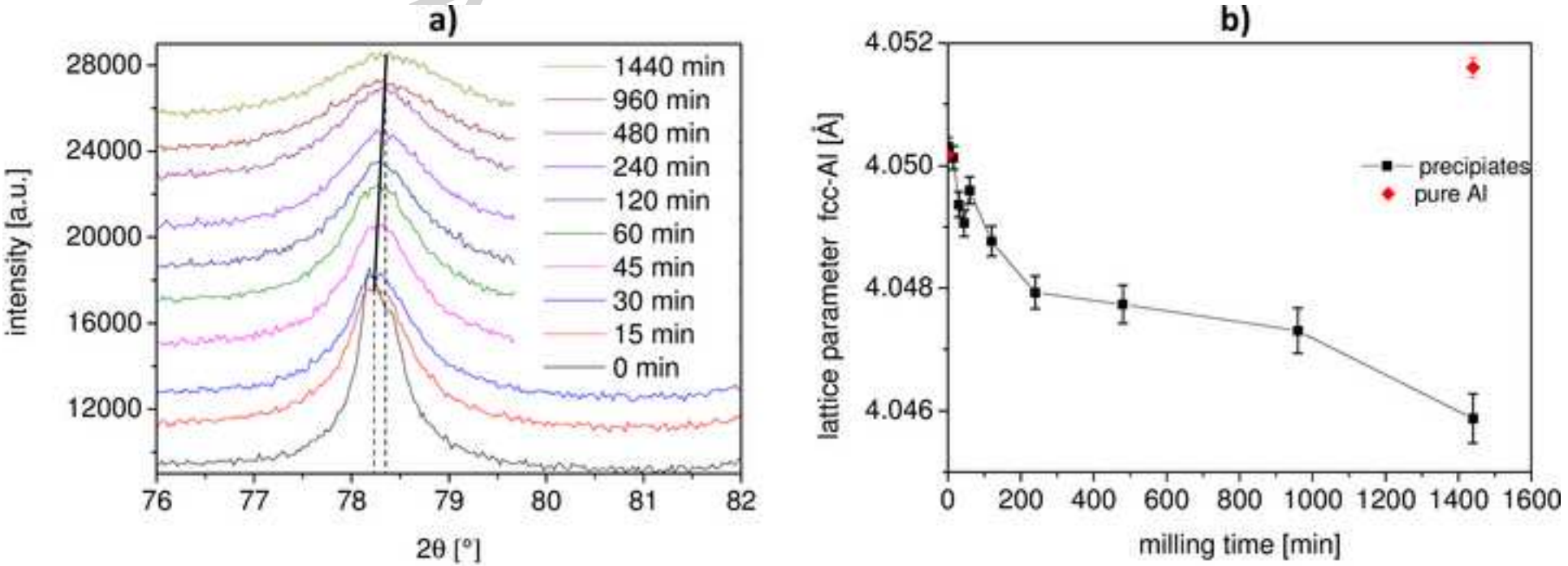

Figure 2: XRD analysis results of fcc-Al precipitates as a function of milling time. (a) (311) reflection shift and broadening (raw data with sample displacement correction from Rietvield refinement) and (b) lattice parameter decrease of fcc-Al precipitates.

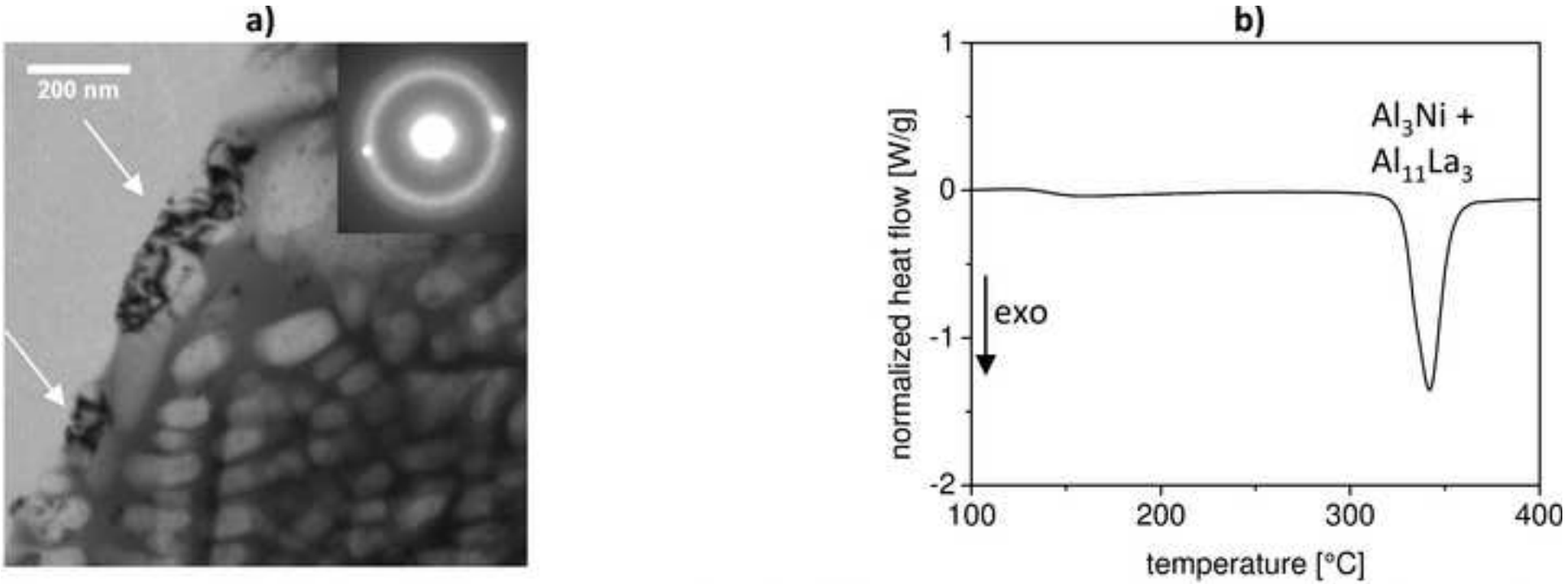

Figure 1: (a) TEM bright field micrograph of a $Al_{87}Ni_8La_5$ powder particle in as-atomized state with the corresponding SAD pattern. Bright fcc-Al crystallites are embedded in the darker amorphous matrix. Artifacts at the interface to the particle (marked by arrows) are visible in the upper left part of the figure. (b) DSC diagram of as-atomized $Al_{87}Ni_8La_5$ powder with a Al_3Ni + $Al_{11}La_3$ crystallization peak.

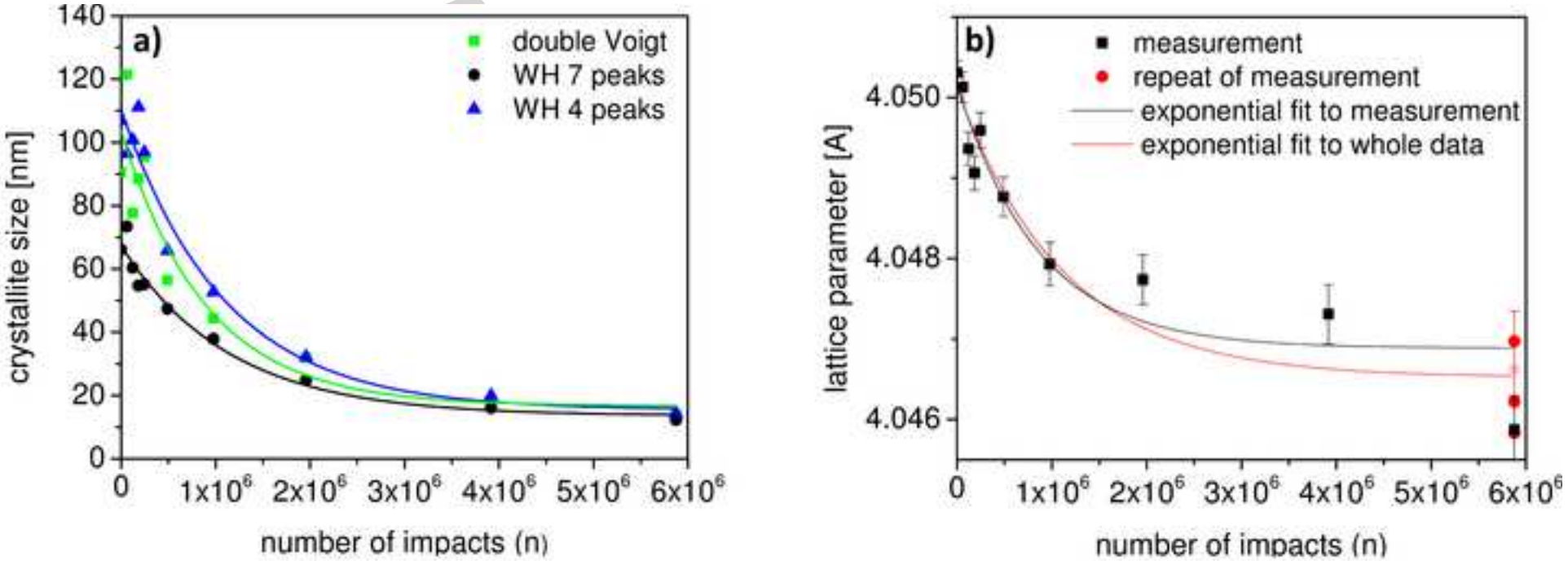

Figure 6: (a) Crystallite size and (b) lattice parameter as a function of the number of impacts n. The data points denote experimentally determined values while the lines are fits to the data. The red colored dots at $5.9 \cdot 10^6$ impacts are taken from a repetition of the measurement with a different diffractometer (different slit size and without sample rotation).